JOURNAL OF THE BALKAN GEOPHYSICAL SOCIETY, Vol. 1, No 2, May 1998, p. 27-37, 15 figs.

Methods for interpretation of synthetically produced archaeomagnetic data

Meliha Dogan[*] and Abdullah Ates[**†]

[*]Department of Archaeometry, Middle East Technical University, 06531,Ankara, Turkey
[**]Ankara Universitesi, Jeofizik Muh. Bol., Besevler 06100, Ankara, Turkey
[†]Corresponding author: E-mail: ates@science.ankara.edu.tr

(Received 15 December 1997; accepted 25 April 1998)

Abstract: *Some variants of the potential field data analysis techniques are discussed in view of the maximum information that could be obtained from an archaeogeophysical survey. The emphasis is given on the computer-based methods of data processing.*

The power spectrum analysis has been used to estimate the depth of known models. A method based on the location of maxima of the horizontal gradient data obtained from the pseudogravity transformation of the theoretical magnetic anomalies has been applied to the synthetic anomalies. The pseudogravity transformation eliminates the distortion caused by orientation of the Earth's magnetic field vector and the effect of the remanence. The locations of maxima of the horizontal gradient of the pseudogravity anomalies have accurately outlined the edges of the causative bodies.

Key Words: *Archaeomagnetic Data, Power Spectrum, Pseudogravity, Locations of Maxima*

INTRODUCTION

Magnetic prospecting is the tool to locate the features that have susceptibility, which differs from that of the surroundings. Induced, and/or remnant magnetisation which may exist in baked clays, such as bricks, tiles, kilns, hearths, cause the distortion of Earth's magnetic field. These distortions can be measured, processed and analysed by means of magnetic prospecting methods.

Tsokas and Rocca (1986), Tsokas and Papazachos (1989) have applied similar processing methods to synthetic and actual magnetic data. Chavez et al. (1995) have used some filtering and spectral methods for the interpretation of the archaeomagnetic data.

The aim of this paper is to test the success of data analysis techniques by the interpretation of synthetic magnetic data obtained from the response of objects buried at 1 and 2 m below the surface. Modern interpretation methods, such as pseudogravity transformation of magnetic anomalies and the method of edge delineation are used (Fig. 1).

PRODUCING SYNTHETIC MAGNETIC ANOMALIES

Figure 2 shows the parameters of a rectangular magnetic body buried at 2 m depth, having dimensions 1x3x1 m (Dogan, 1996). Figure 3 shows the plane and sectional view of a body having a kiln-like shape and another rectangular prism at 1 and 2 m depth, with dimensions 3x3x1 m and 1x2x1 m respectively. The models were considered as located underneath a 19x19 m measuring grid. The calculated anomalies of these models are shown in Fig.4 and 5. No remanent magnetisation was considered.

The parameters of the models are shown in Tables 1 and 2. Magnetic anomalies were also calculated for the same models including remanent magnetisation; these are shown in figures 6 and 7. The parameters of those models, where remanence was taken into account are listed in Tables 3 and 4. All the synthetic effects were produced using the computer program "prism" written by Kearey(1977) using the Goodacre's(1973) algorithm for 1 m sampling interval covering the survey area of 19x19 m.

The magnetic anomalies of the models appear to be shifted because of the vector orientation of the Earth's magnetic field (Fig. 4 and 5). A further deterioration seems to be observed because of the remanent magnetisation included into the models 1 and 2 (Fig.6 and 7).

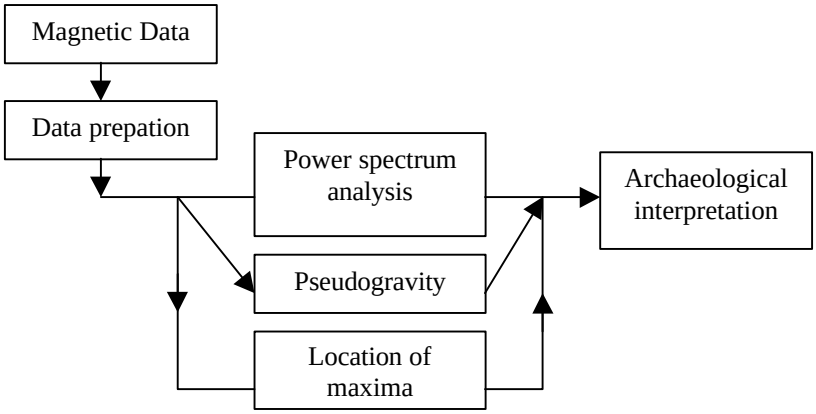

Figure 1. The processing steps of the digital magnetic data.

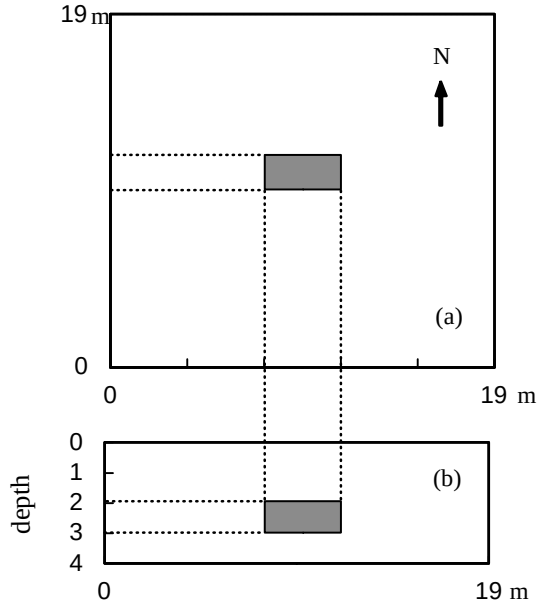

Figure 2. Model 1 (a-plan view, b-sectional view) which used to produce the magnetic anomalies. Horizontal dimensions are 1x3 m2 and its depth extent is 1 m; ρ = 2 Mg m $^{-1,}$ J= 1 A m $^{-1}$.

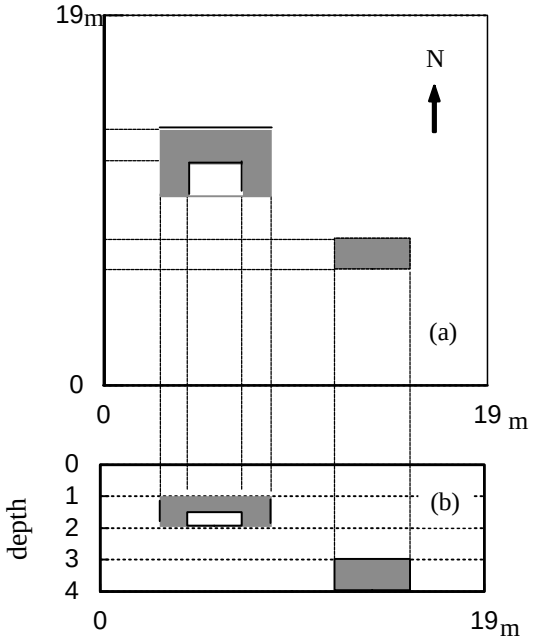

Figure 3. Model 2 and 3 (a-plan, b-section) used to produce the magnetic anomalies. A kiln-like object and another object with dimensions of 3x3x1 m and 2x1x1 m. ρ = 2 Mg m $^{-1,}$ J= 1 A m $^{-1}$.

Table 1. Parameters of the synthetic model 1.

Size		Inclination		Declination		Density contrast	Intensity of magn.
Burial depth	Thickness	Earth	Body	Earth	Body	Mg m^{-3}	A m^{-1}
2 m	1 m	55° N	55° N	4° N	4° N	2	1

Table 2. Parameters of the synthetic model 2 and model 3.

Size		Inclination		Declination		Density contrast	Intensity of magn.
Burial depth	Thickness	Earth	Body	Earth	Body	Mg m^{-3}	A m^{-1}
1 m	1 m	55° N	55° N	4° E	4° E	2	1
2 m	1 m	55° N	55° N	4° E	4° E	2	1

Table 3. Parameters of the synthetic model 1 including remanent magnetization.

Size		Inclination		Declination		Density contrast	Intensity of magn.
Burial depth	Thickness	Earth	Body	Earth	Body	Mg m^{-3}	A m^{-1}
2 m	1 m	55° N	55° N	4° E	-55° W	2	1

Table 4. Parameters of the synthetic model 2 and model 3 including remanent magnetization.

Size		Inclination		Declination		Density contrast	Intensity of magn.
Burial depth	Thickness	Earth	Body	Earth	Body	Mg m^{-3}	A m^{-1}
1 m	1 m	55° N	55° N	4° E	-45° W	2	1
2 m	1 m	55° N	55° N	4° E	4° E	2	1

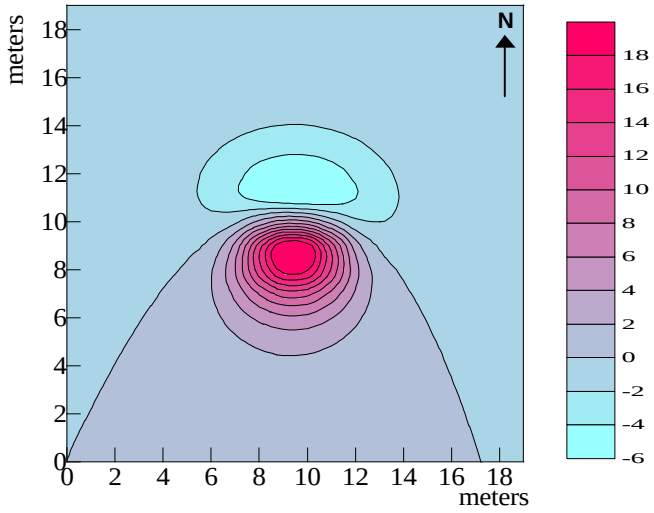

FIG. 4. Magnetic anomalies (nT) of the model shown in Fig.2. Inclination and declination of the Earth's magnetic field are 55°N and 4° E. Inclination and denclination of body magnetisation are 55° N and 4° E also.

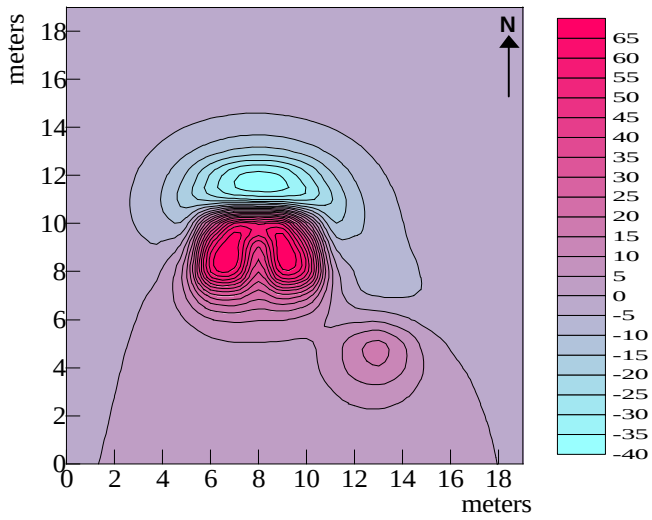

FIG. 5. Magnetic anomalies (nT) of the models shown in Fig.3. Inclination and declination of the Earth's magnetic field are 55° N and 4° E. Inclination and declination of bodies' magnetisation are 55° N and 4° E also .

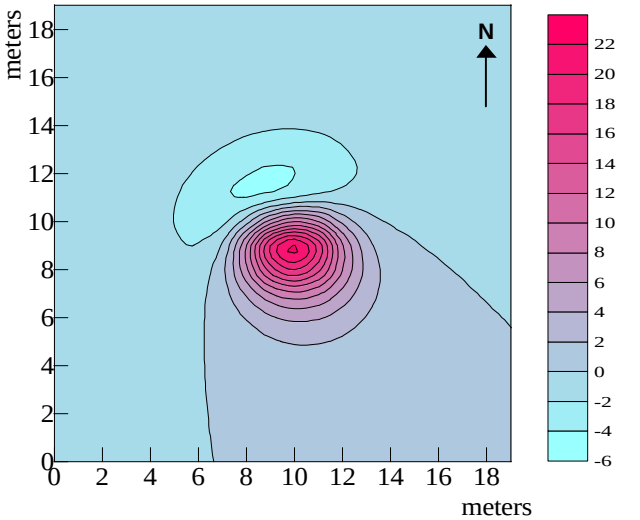

FIG. 6. Magnetic anomalies (nT) of the models shown in Fig.2 including remanent magnetisation. Inclination and declination of the Earth's magnetic field are 55°N and 4°E. Inclination and declination of body magnetisation are 55° NW and -55°W .

POWER SPECTRUM ANALYSIS

The depth of a magnetically disturbing body or an ensemble of bodies can be estimated from the wavenumber spectrum of the associated anomaly. The power spectrum analysis reveals the presence of magnetic sources and gives estimation about the approximate depths (Spector and Grant, 1970). The data are transformed into the frequency domain and its 2D power spectra are rearranged to be centred at the middle point of the array. Spector and Grant (1970) give the azimuthally averaged power spectrum of an ensemble of rectangular blocks by the following equation

$$P = [\exp -4\pi h][(1-\exp(2\pi k t))^2][S^2(k,\theta)], \quad (1)$$

where h and t are the depth to the top of a prism and its thickness, respectively. S is a function and depends on the horizontal dimensions of the prism. The square brackets represent the effects of azimuthal and ensemble averaging. A simplified formula can be derived by ignoring the size of the bodies and leads to modelling of the spectrum by a distribution of point sources. In this case, an estimate of the maximum possible depth ($\bar{h}$) can be obtained from the expression given below

$$\frac{\Delta \log_e P}{\Delta k} = -4\pi\bar{h}; \quad (2)$$

The depth estimation of buried bodies can be carried out by using the gradient of linear segment in the graph of $\log_e P$ versus the wave number k. Since the size of a causative body is ignored, the calculated depth using this relationship will represent a maximum estimate (Spector and Grant, 1970).

Figure 8a and b show the graph of $\log_e P$ versus k whose slope helps to obtain depth estimation. Depths to the top of the anomalous synthetic bodies have been calculated using the equation (2). The calculated depths for the models 1, 2 and 3 are 1.99, 0.91 and 1.78 meters, respectively.

The estimated depth of the model 1 buried at 2 m is calculated as 1.99 m by using the power spectrum technique (Dogan, 1996). The calculated depths for model 1 and 2 are 0.91 m and 1.78 m. Those depth estimations are approximately consistent with the true depths that are 1 m and 2 m, respectively. These results reveal that the power spectrum analysis can be used for the depth estimation of shallow buried targets with confidence, although the calculated depth for model 3 slightly differs from the true one.

PSEUDOGRAVITY TRANSFORMATION

Interpretation of magnetic anomalies is more difficult in comparison with the gravity anomalies. In general, a simple connection may exist between the gravity anomalies and causative bodies. However, the Earth's magnetic field distorts the magnetic anomalies. For this reason, the apex of the magnetic anomalies is shifted with respect to the projection of the corresponding sources to the surface. The indirect interpretation of magnetic data using the transformed pseudogravity data is easier than the direct interpretation of magnetic anomalies (Kearey and Brooks, 1991). This type of transformation has been first applied by Baranov (1957) and progressively developed by many researchers in the subsequent years.

The Poisson equation can be used to transform magnetic fields into gravitational fields. This is

$$V = \frac{J}{G\rho} \cdot \frac{\partial U}{\partial v}, \quad (3)$$

where V is the magnetic potential due to a magnetised body in the direction v with an intensity of magnetisation J, U is the gravitational potential of the same body with uniform density, G is the international gravitational constant. If a conventional density, $r = J/G$ is inserted into equation (3), one finds

$$V = \frac{\partial U}{\partial v}, \quad (4)$$

The differentiation of the above equation with respect to Z gives

$$Z = \frac{\partial g}{\partial v}, \quad (5)$$

where g is not the true gravity anomaly and consequently it was named as the "*pseudogravimetric anomaly*". Because, the true density variation in the subsurface is not known and unmagnetised bodies could not contribute to the potential U. Then, the vertical component Z of the magnetic anomaly is expressed in terms of the derivative of the pseudogravimetric anomaly (Baranov, 1957).

If the body is magnetised vertically, Z will be equal to total field. Consequently, the first vertical derivative of the pseudogravimetric anomaly will be equal to the transformation of total magnetic field to the magnetic pole. Then, this transformation will eliminate the asymmetry and lateral displacement of the magnetic anomaly with respect to apex of the causative body. Since the magnetic field is vertical at the North magnetic pole, a transformed total field anomaly looks as if it was observed at this region (Chavez et al., 1995).

The algorithm of Blakely and Simpson (1986) has been used for the calculation of pseudogravity data. The ratio of J/r is set to unity in this algorithm. The

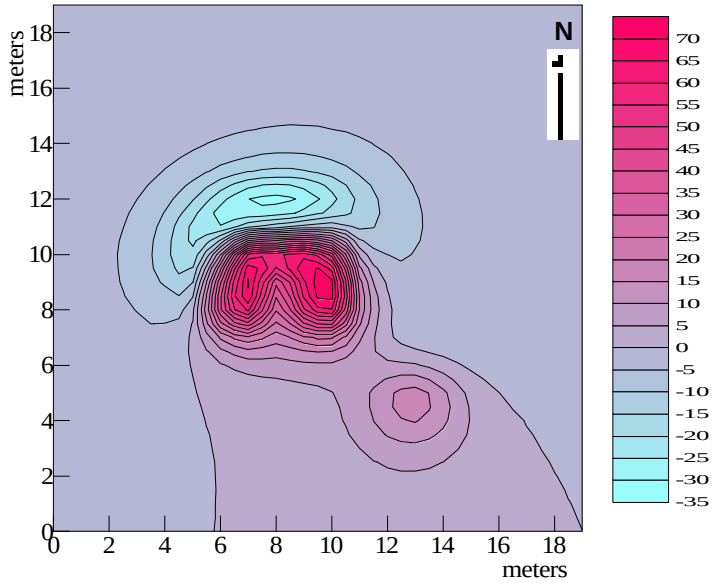

FIG. 7. Magnetic anomalies (nT) of the models shown in Fig.3 including remanent magnetisation. Inclination and declination of the Earth's magnetic field are 55° N and 4° E. Inclination and declination of bodies magnetisation are 55° NW and -45° W, 55° NW and 4° E.

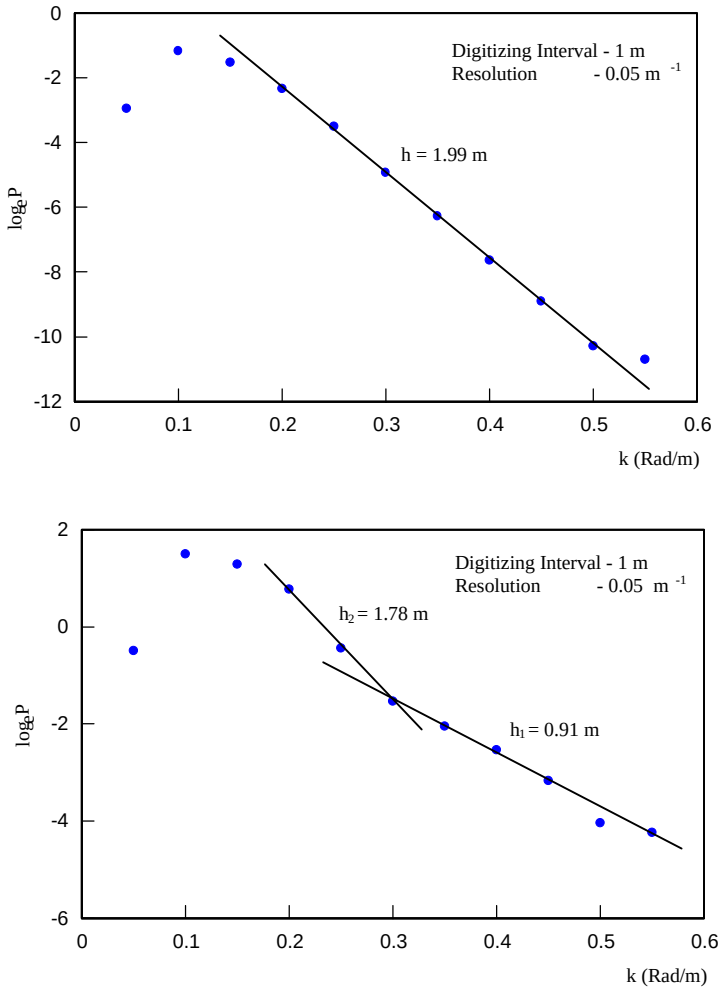

FIG.8.(a) Plot of the azimuthally averaged power spectrum (Log_e P) versus wavelength (k) for magnetic anomalies shown in Fig.4. Estimated depth to the top of the model 1 is shown in Fig.4 as 1.99 m. (b) Plot of the azimuthaly averaged power spectrum (Log_eP) versus wavelength (k) for magnetic anomalies shown in Fig 5. Estimated depth to the top of the model 2 is shown in Fig.5 as 0.91 m and to the top of model 3 is 1.78 m.

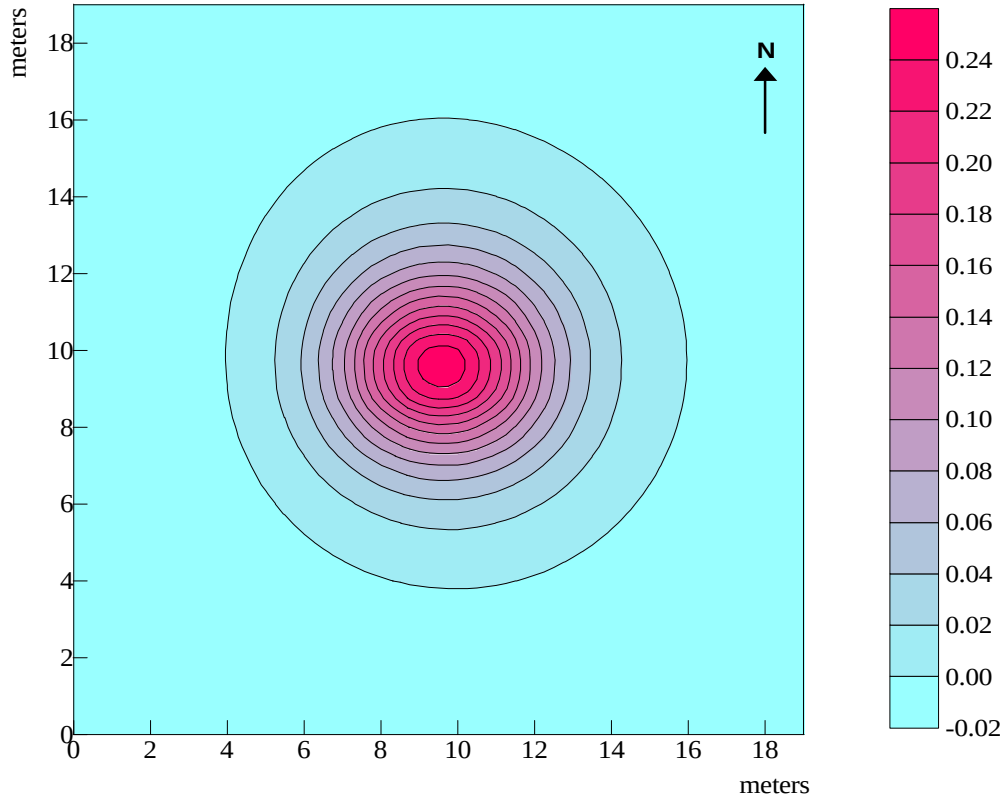

FIG. 9. Pseudogravity anomaly of the field shown in Fig.4. Inclination and denclination of the magnetisation vector are 55° N and 4° E. Counter interval is 0.02 mgal.

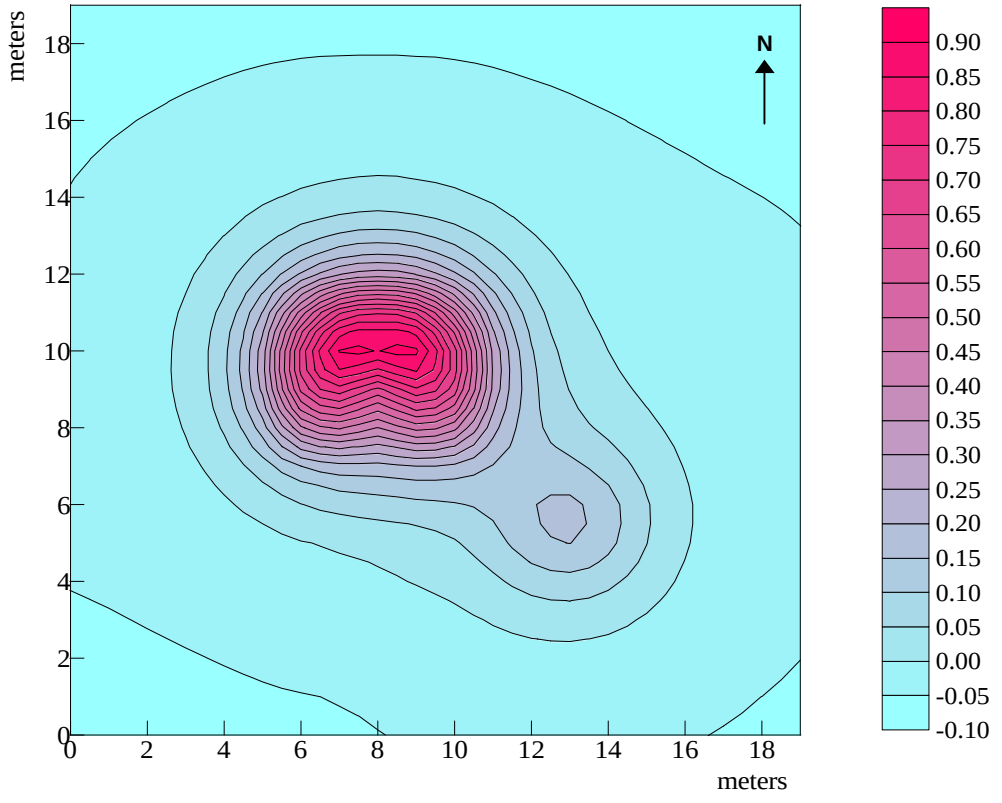

FIG.10. Pseudogravity anomaly of the field shown in Fig.5. Inclination and denclination of magnetisation are 55° N and 4° E. Counter interval is 0.05 mgal.

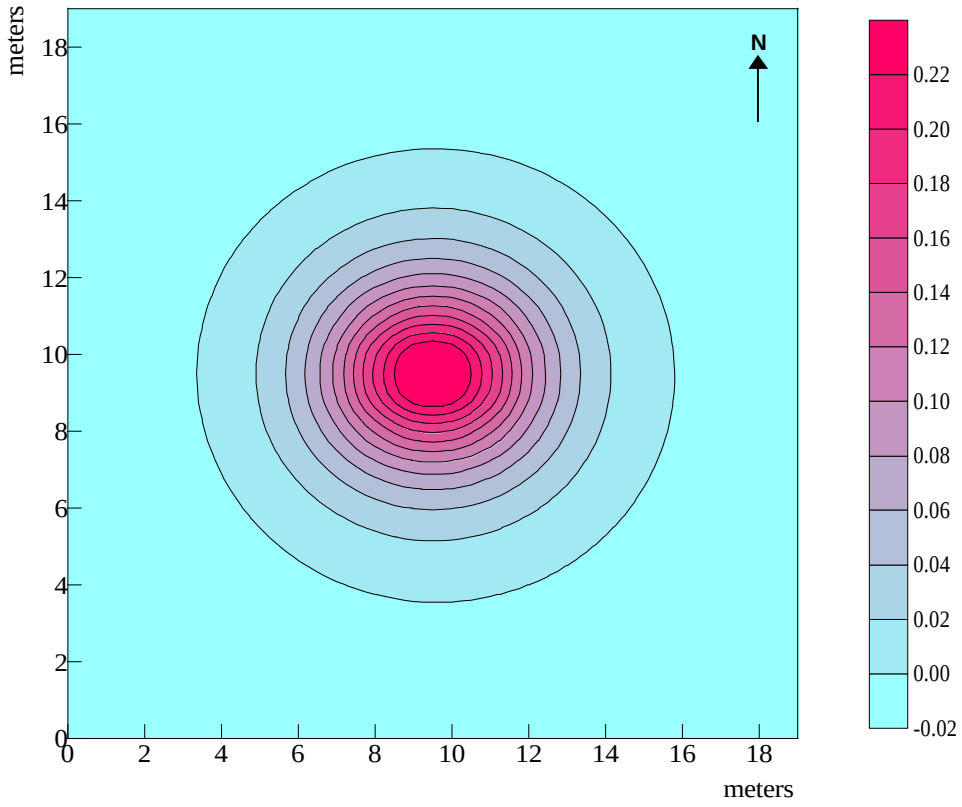

FIG.11. Pseudogravity anomaly of the field shown in Fig.6 which includes the remanent magnetisation effect. Inclination of the Earth's magnetic field and body magnetisation is 55°N. Declination of the Earth's magnetic field and body magnetisation is 55°N. Declination of the Earth's magnetic field and body magnetisation are 4°E and 55°W, respectively. Counter interval is 0.02 mgal.

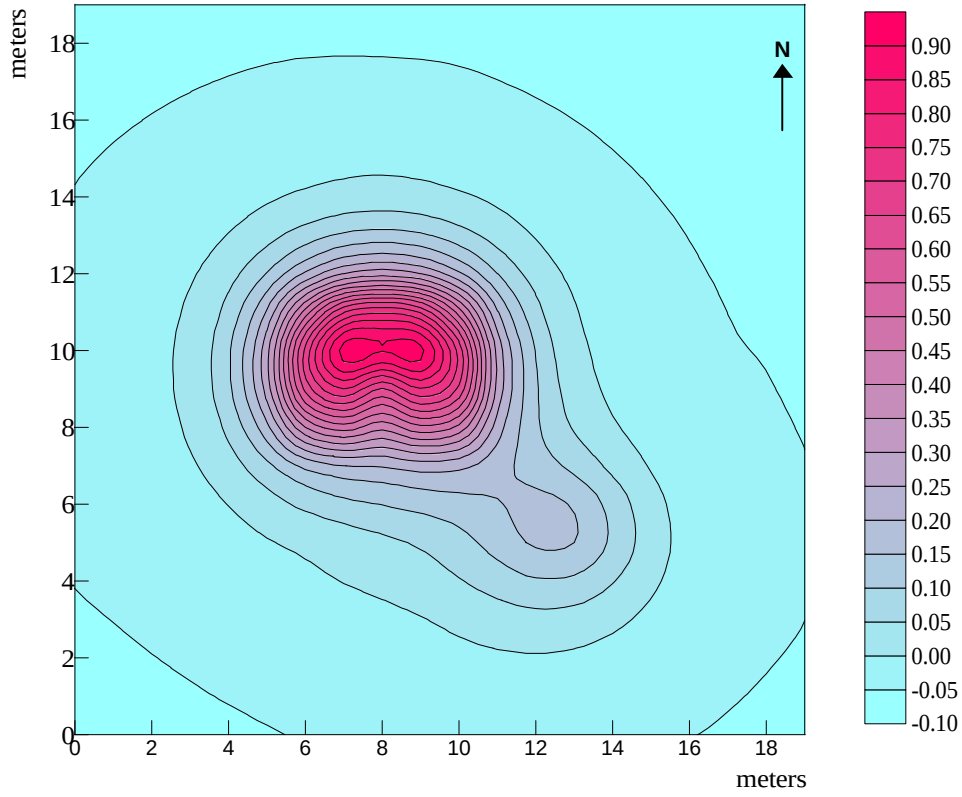

FIG.12. Pseudogravity anomaly of the field shown in Fig.7 which includes the remanent magnetisation effect. Inclination and denclination of the Earth's magnetic field are 55°N and 4°E, respectively. Inclination and denclination of bodies are 55°NW and -45°W, 55°NW and 4°E, respectively. Counter interval is 0.05 mgal.

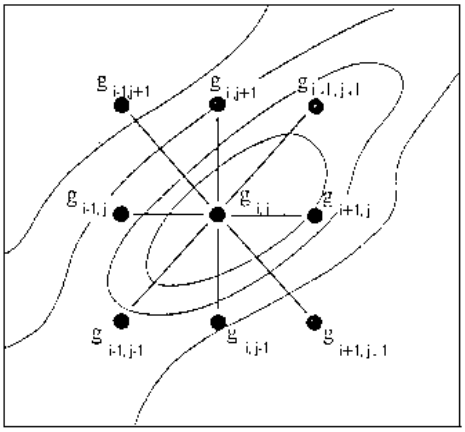

FIG. 13. The grid nodes lay out on the map of the horizontal gradient of magnetic anomalies, which is used to find whether a maximum is present around $g_{i,j}$ (Blakely and Simpson, 1986).

pseudogravity transformation has produced anomalies in which the asymmetry and lateral displacement of magnetic anomalies are eliminated (Fig. 9 and Fig. 10).

In the first case, it is assumed that the models are megnetised along the earth magnetic field. The second case consists of the model 1 and 2 that are remanently magnetised with the angles of I=55°, D=-55° and I=55°, D=-45°, respectively. Figures 11 and 12 show the pseudogravity anomalies computed for both cases.

It is worthy to note that the displayed distortion has been removed and the apexes of the anomalies fit with the centre of the models in either induced and remanent field cases. Therefore, it can be concluded that the use of this method removes the effects of remanent magnetisation and makes the interpretation of magnetic anomalies easier.

SEARCHING FOR MAXIMA

Cordell and Grauch(1985) presented a method for locating edges of magnetic bodies. Blakely and Simpson (1986) automated the technique to make possible a rapid interpretation of horizontal gradient magnitudes. The method consists of three steps, namely a) pseudogravity transformation, b) calculation of the magnitude of the horizontal gradient of the pseudogravity anomaly, c) contouring the maximum horizontal gradient

Each grid node $g_{i,j}$ is compared to its eight nearest neighbours in four directions and the maxima of the measured field are found (Fig.13). The following inequalities are tested during the comparison.

$$g_{i-1,j} < g_{i,j} > g_{i+1,j} \quad (6)$$

$$g_{i,j-1} < g_{i,j} > g_{i,j+1} \quad (7)$$

$$g_{i+1,j-1} < g_{i,j} > g_{i-1,j+1} \quad (8)$$

and

$$g_{i-1,j-1} < g_{i,j} > g_{i+1,j+1} \quad (9)$$

For each satisfied inequality a counter N is increased by one. N varies in the range from 0 to 4 and provides a measure of the quality of maximum. Therefore, it is called as "significant level " of the maximum (Blakely and Simpson, 1986).

Lets assume that $g_{i-1,j} < g_{i,j} > g_{i+1,j}$ is satisfied and the horizontal location of the maximum relative to the position of $g_{i,j}$ given by

$$x_{max} = \frac{bd}{2a} , \quad (10)$$

where

$$a = \frac{1}{2}[g_{i-1,j} - 2g_{i,j} + g_{i+1,j}] , \quad (11)$$

$$b = \frac{1}{2}[g_{i+1,j} - g_{i-1,j}] , \quad (12)$$

and d is the distance between grid nodes. The value of the maximum horizontal gradient at x_{max} is given by

$$g_{max} = ax_{max}^2 + bx_{max} + g_{i,j} . \quad (13)$$

If more than one inequality are satisfied then the largest g_{max} and corresponding x_{max} is selected as appropriate maximum for that grid node.

This method doesn't require an assumption about the source except the direction of magnetisation. The derived maxima approximately delineate the edges of a shallow magnetic source having abrupt and nearly vertical contact. It is obvious that the method can correctly predict the shape of the magnetic source, but it tends to round up the corners. The method does not work accurately for the sources with nonvertical

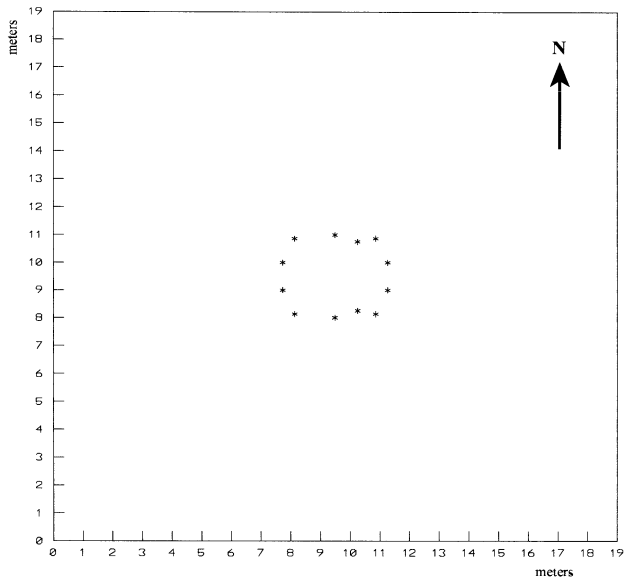

FIG. 14. Location of maxima of the horizontal gradient of the pseudogravity anomaly shown in Fig.9.

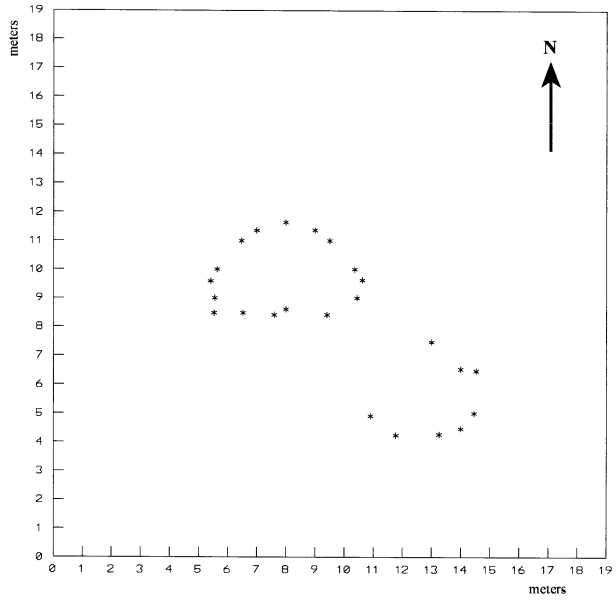

FIG. 15. Location of maxima of the horizontal gradient of the pseudogravity anomaly shown in Fig.10.

contacts but it gives good results for sources sources having certain geometric shapes.

The computations are applied in three sequential steps calculation of the pseudogravity anomaly, derivation of the horizontal gradient and finally estimation of the maxima of horizontal gradient. Those can be done by the selection of a suitable significance level. Various "significant levels" for the “location of maxima" in the third step were examined to find out a good estimation for the geometrical distribution of the causative model. The significance level "3” has found to be the best one for this purpose and used for the computation.

A reasonable resemblance between the shape of models and derived borders obtained by the use of this method (Fig. 14 and 15).

CONCLUSION

The application of advanced magnetic prospecting methods on synthetically produced magnetic anomalies was presented.

Depths to the tops of the models from surface were accurately calculated by the spectral slope technique wherever the concealed bodies are big enough. However, lack of accuracy is obtained for bodies whose dimensions are comparable to the wavelength as expected.

Pseudogravity transformation makes the interpretation easier while the horizontal gradient maxima delineate their edges. Therefore, the techniques considered are suitable for the geophysical exploration of archaeological sites.

REFERENCES

Baranov, V., 1957, A new method for interpretation of aeromagnetic maps: pseudo-gravimetric anomalies: Geophysics, **22**, 359-383.

Blakely, R.J., and Simpson, R.W., 1986, approximating edges of source bodies from magnetic or gravity anomalies: Geophysics, **51**, 1494-1498.

Chavez, R.E, Hernandez, M.C, Herrera, J., and Camara, M.E., 1995, A magnetic survey over La Maja, an archaeological site in northern Spain: Archaeometry, **37**, 171-184.

Cordell, L. and Grauch, V.J.S, 1985, Mapping basement magnetization zones from aeromagnetic data in the San Juan basin, New Mexico, in Hinze, W.J., ed., The utility of regional gravity and magnetic anomaly maps: Soc. Exploration Geophysics, Tulsa, Oklahoma, 181-197.

Dogan, M., 1996 Magnetic prospecting in Kocumbeli arch-aeological site: METU Campus, Ankara, Turkey. M.Sc. Thesis, Department of Archaeometry, METU, Ankara.

Goodacre, A. K., 1973. Some comments on the calculation of the gravitational and magnetic attraction of a homogeneous rectangular prism, Geophysical Prospecting, **21**, 66-69.

Kearey, P., and Brooks, M., 1991, An introduction to geophysical exploration: Blackwell Scientific Publications.

Spector, A., and Grant, F.S., 1970, Statistical models for interpreting aeromagnetic data: Geophysics, **35**, 293-302.

Tsokas, G.N., and Rocca, A.Ch., 1986, Geophysical prospecting at archaeological sites with some examples from northern Greece, First Break, **4**, 31-39.

Tsokas, G., and Papazachos, C.B., 1992. Two-dimensional inversion filters in magnetic prospecting: Application for buried antiques, Geophysics, **58**,1004-1013.